

# ADVANCED FUNCTIONAL MATERIALS

## Supporting Information

for *Adv. Funct. Mater.*, DOI: 10.1002/adfm.202003851

### Inverse Solidification Induced by Active Janus Particles

*Tao Huang, Vyacheslav R. Misko, Sophie Gobeil, Xu Wang,  
Franco Nori, Julian Schütt, Jürgen Fassbender, Gianaurelino  
Cuniberti, Denys Makarov,\* and Larysa Baraban\**

## Supporting Information

### Inverse Solidification Induced by Active Janus Particles

*Tao Huang<sup>1,6</sup>, Vyacheslav R. Misko<sup>2,3</sup>, Sophie Gobeil<sup>1</sup>, Xu Wang<sup>4</sup>, Franco Nori<sup>2,5</sup>, Julian Schütt<sup>1,4</sup>, Jürgen Fassbender<sup>4</sup>, Gianaurelio Cuniberti<sup>1</sup>, Denys Makarov<sup>4\*</sup>, Larysa Baraban<sup>1,6\*</sup>*

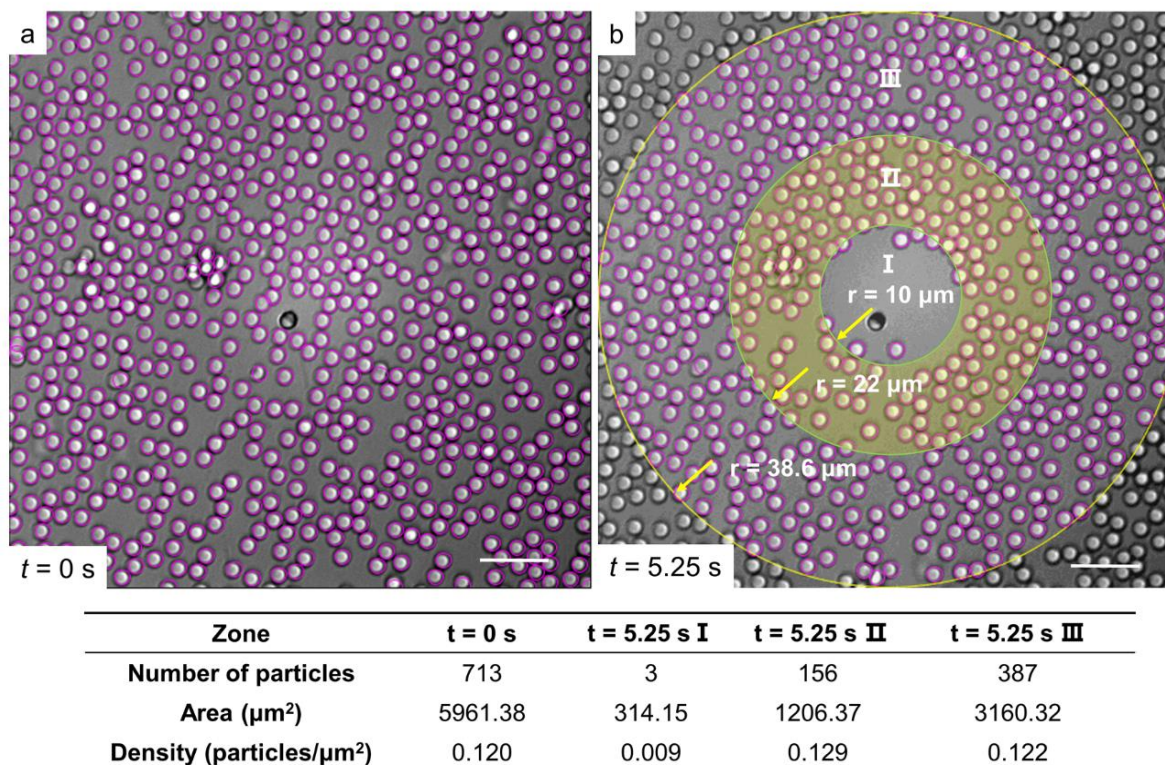


**Figure S1.** Calculation of the areal density of passive beads within the region of interest for the case of a single active defect illuminated with blue light. (a) Initial distribution of passive beads (illumination time  $t = 0$  s). All passive beads in the field of view are taken into account for the calculation of the areal density and are indicated with violet circles. Scale bar,  $10 \mu\text{m}$ . (b) Distribution of passive beads illuminated with blue light for  $t = 5.25$  s. Density of passive beads is calculated in different regions of interest (indicated by colors). The highest density is in the yellow-shaded region. Scale bar,  $10 \mu\text{m}$ . The images are frames of the Movie S1.

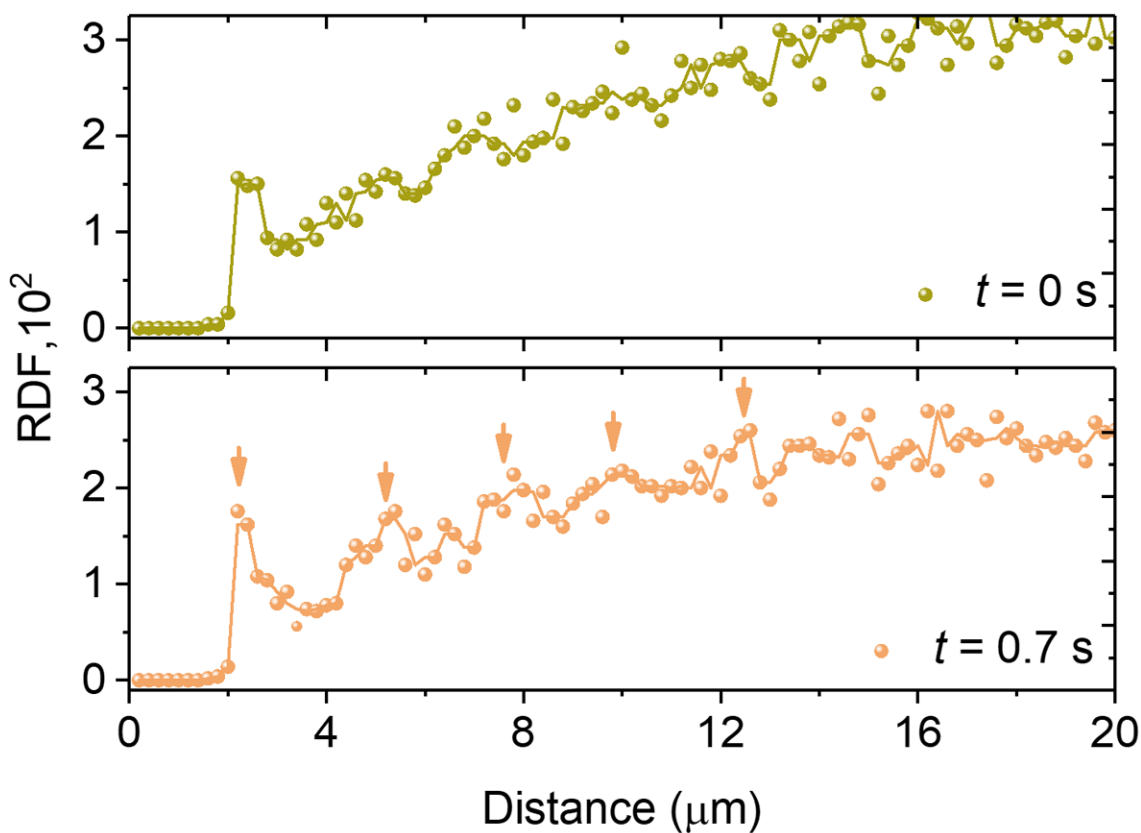


**Figure S2.** The radial distribution function (RDF) for the case of a single active defect in a matrix of passive beads. The RDF is calculated from the frames of the Movie S1 taken at (top panel)  $t = 0$  and (bottom panel)  $t = 0.7$  s. The corresponding microscopy images are shown in the main text, Figure 2. The initial RDF at  $t = 0$  s shows only one peak followed by a featureless signal that is indicative of an amorphous state in the system. The appearance of discrete peaks (indicated with orange arrows) for  $t = 0.7$  s indicates the onset of long-range order.

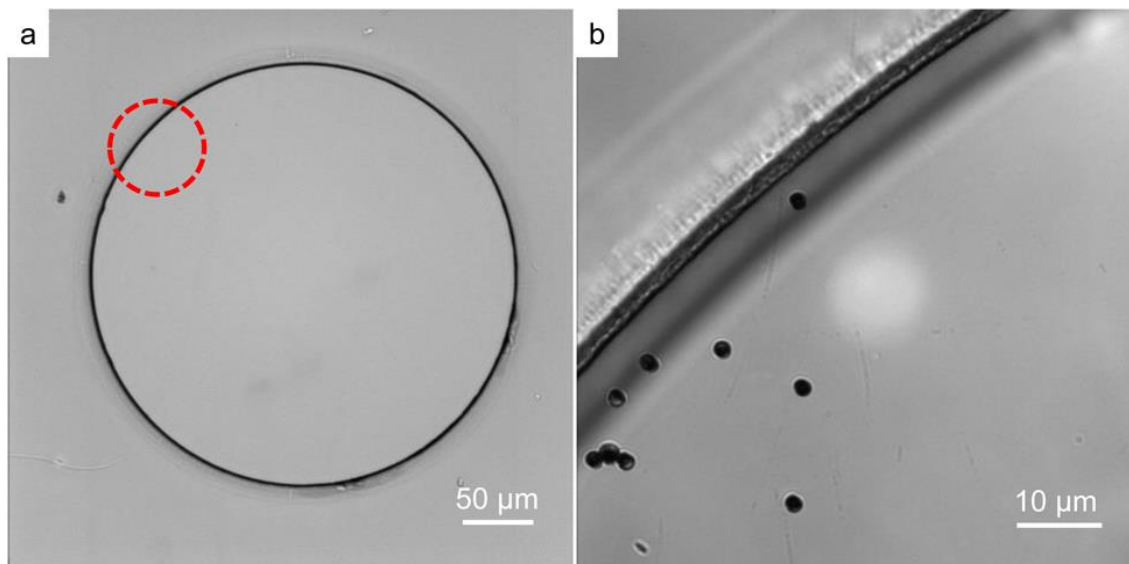


**Figure S3.** (a) Optical microscopy image of a single microwell. A circular structure (15  $\mu\text{m}$  high and 300  $\mu\text{m}$  diameter) was fabricated using a negative photoresist on a glass substrate. (b) Close-up of the panel (a) in the region indicated with dashed red circle. Several Janus particles (black circular objects) can be seen inside the microwell.

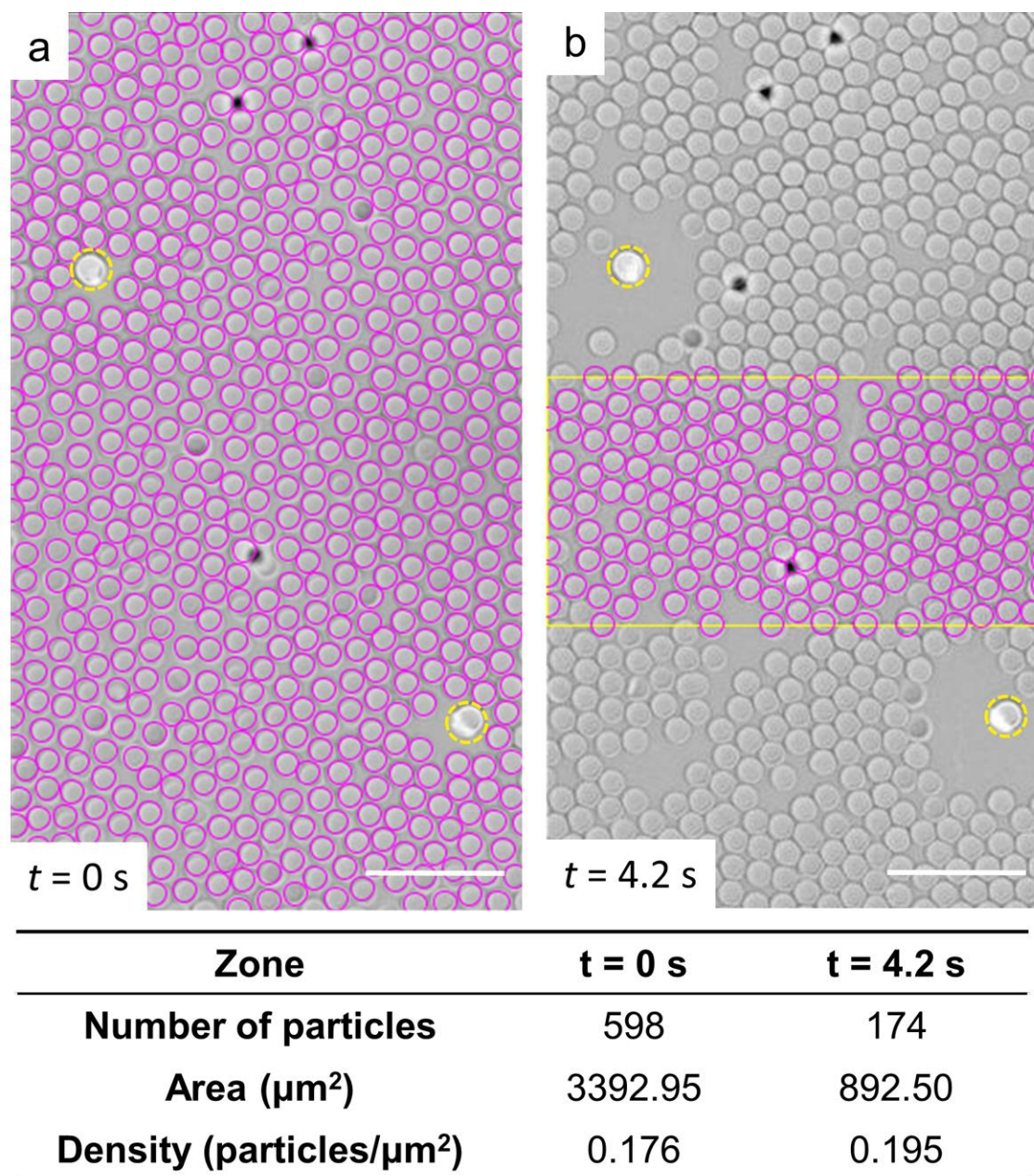


**Figure S4.** Calculation of the areal density of passive beads within the region of interest (particles indicated with violet circles) for the case when the system contains low concentration of Janus particles (2 active defects). The images are frames of the Movie S2. (a) Initial distribution of passive beads ( $t = 0 \text{ s}$ ). Scale bar,  $10 \mu\text{m}$ . (b) Arrangement of particles in the system after  $t = 4.2 \text{ s}$ . Scale bar,  $10 \mu\text{m}$ .

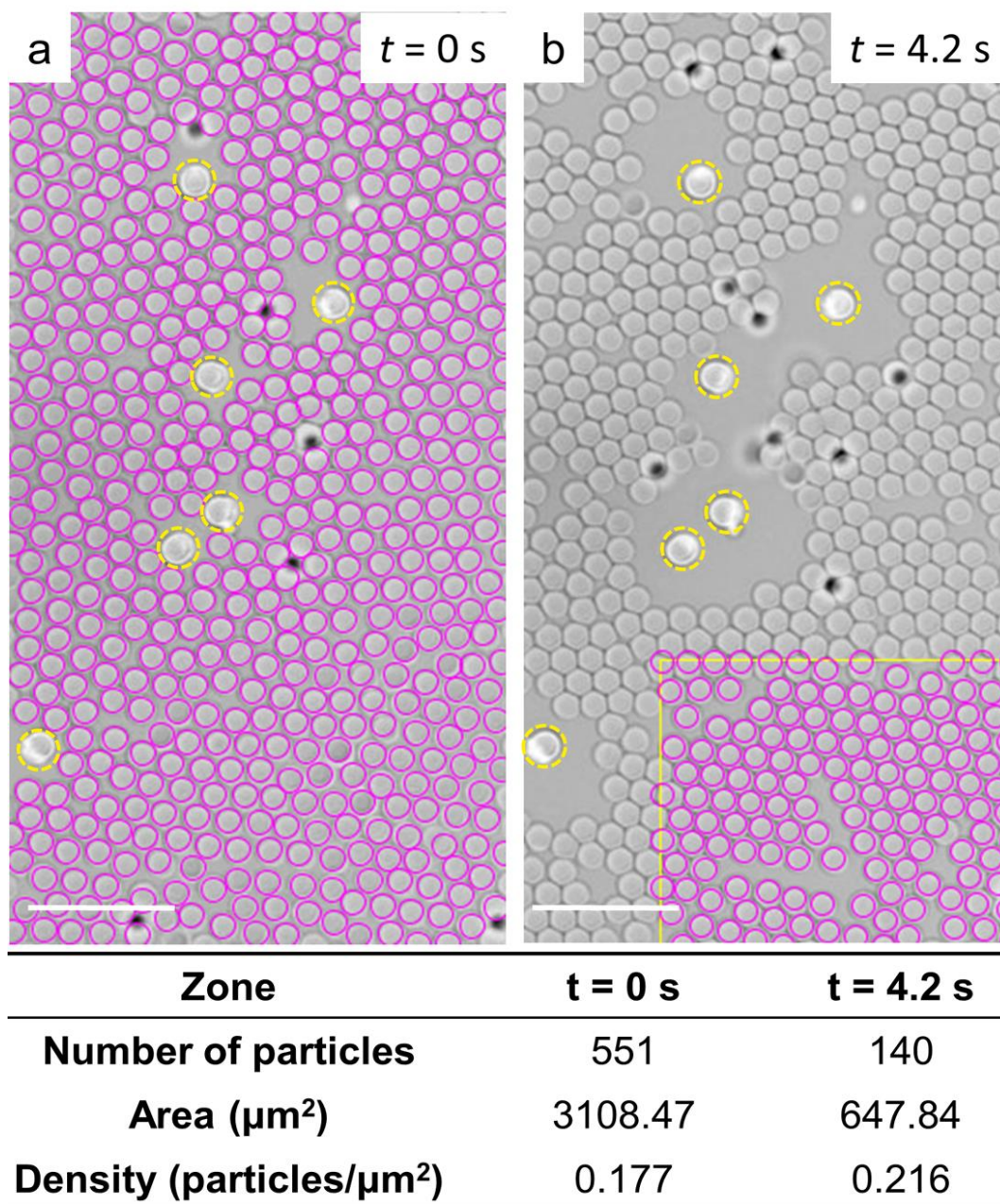


**Figure S5.** Calculation of the areal density of passive beads within the region of interest (particles indicated with violet circles) for the case when the system contains high concentration of Janus particles (6 active defects). The images are frames of the Movie S3. (a) Initial distribution of passive beads ( $t = 0 \text{ s}$ ). Scale bar,  $10 \mu\text{m}$ . (b) Arrangement of particles in the system after  $t = 4.2 \text{ s}$ . Scale bar,  $10 \mu\text{m}$ .

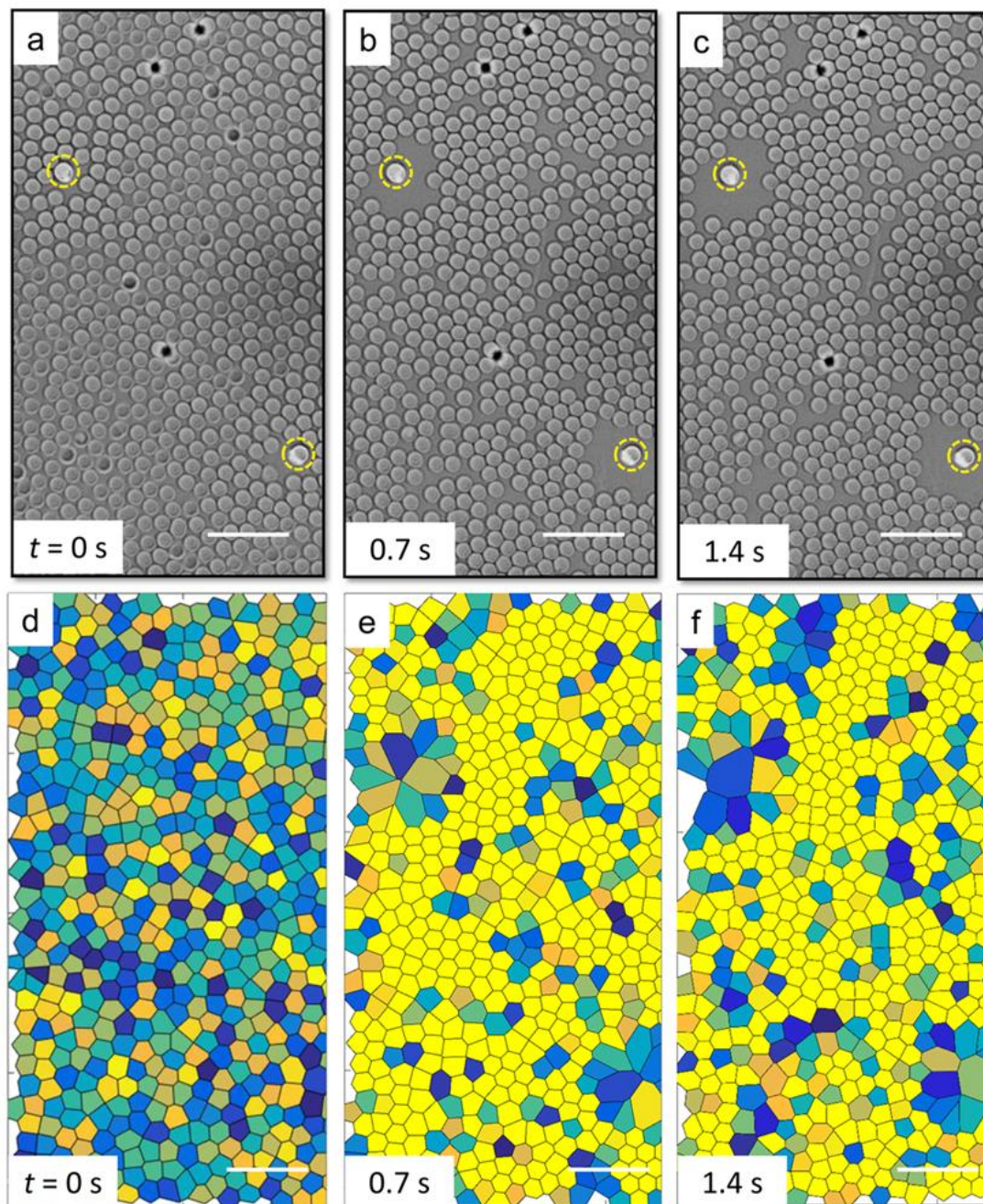


**Figure S6.** (a-c) A sequence of optical microscopy images showing the impact of 2 active defects (indicated with yellow dashed circles) on the initially amorphous matrix of passive silica beads. Scale bar,  $10\ \mu\text{m}$ . The images are frames of the Movie S2. (d-f) Voronoi diagrams illustrating the emergence of the crystalline order under blue light illumination. Scale bar,  $10\ \mu\text{m}$ .



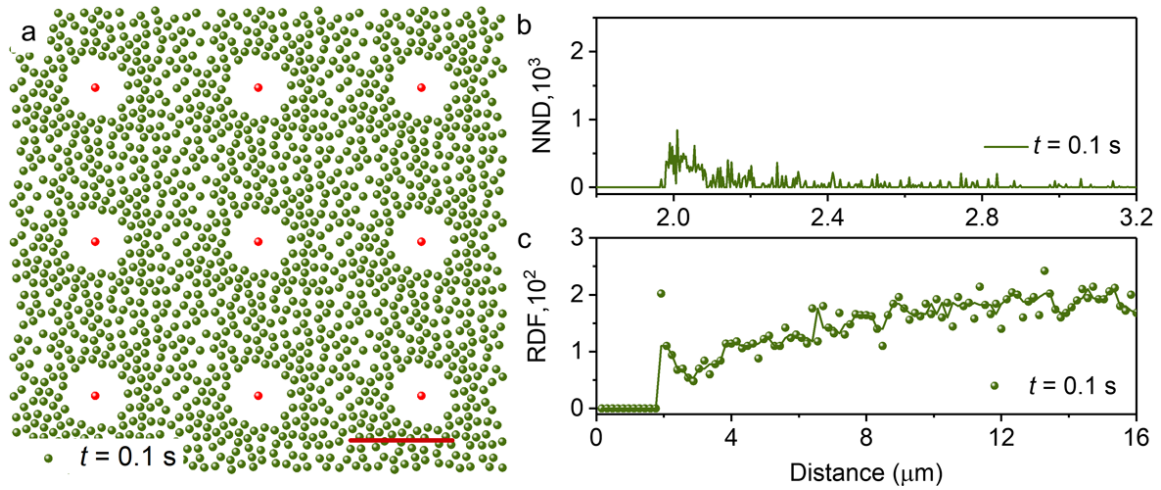


**Figure S7.** Simulation data. (a) Distributions of passive beads in the presence of active defects (shown for one simulation cell and eight images). The snapshot is taken at  $t = 0.1$  s. Scale bar, 20  $\mu\text{m}$ . The corresponding NND and RDF are shown as panels (b) and (c), respectively. At initial stages of the exclusion process ( $t = 0.1$  s), passive beads are compressed in the vicinity of Janus particles. The RDF shows only the first peak, and the NND peak is very weak and broad.

**Supplementary Notes**

**Supplementary Note 1: Mechanisms of exclusion behavior.** Janus particles are composed of a polystyrene sphere (diameter of 2  $\mu\text{m}$ ) covered by Ag/AgCl caps, with nano-particulate structure of the cap.<sup>[1]</sup> When dispersed in deionized water and under blue light illumination (wavelength of 450-470 nm and intensity 137  $\mu\text{W mm}^{-2}$ ), due to the coupling of the plasmonic light absorption by Ag/AgCl cap,<sup>[2]</sup> AgCl is reduced to Ag producing protons and chloride ions. Because protons have a significantly higher diffusivity than chlorine ions ( $D_{\text{H}^+} = 9.311 \times 10^{-5} \text{ cm}^2 \text{ s}^{-1}$  versus  $D_{\text{Cl}^-} = 1.385 \times 10^{-5} \text{ cm}^2 \text{ s}^{-1}$ ) a local electric field around the particle is generated.<sup>[3]</sup> In the far field, this electric field points towards the surface of the cap of Janus particles.<sup>[4]</sup> This electric field acts phoretically on negatively charged  $\text{SiO}_2$  beads (diameter 2  $\mu\text{m}$ ) by pulling them away from Janus particles.

**Supplementary Note 2: Voronoi diagram.** Voronoi cells have a rich history of use in the characterization and analysis of soft matter systems.<sup>[5]</sup> These diagrams are extensively used to characterize phase transitions in colloidal systems, e.g. melting and crystallization, via the statistical information about nearest neighbors in the colloidal network. Here, we briefly summarize how the Voronoi diagrams are used to describe the transient regime from the amorphous to the crystalline state. The yellow colored cells indicate the fractions containing colloidal beads assembled into a crystalline hexagonal lattice. The other colors (blue, orange, green) indicate the cells at the crystalline phase edges and

amorphous fractions of the colloidal matrix, *e.g.* having five/seven nearest neighbors or six with an imperfect geometry.

**Supplementary Note 3: Mobile active defects in dense matrix.** Active defects can induce the liquid to solid transition even if they move. When the density of active defects is low (similar to the static case), the motile active defects induces the 2D shape patterning along the locomotion with exclusion behavior (Movie S4 and Movie S5). Once Janus particle moves far away from its initial position, the colloidal matrix starts to relax back to its initial state. In the case when several active defects moving close to each other (similar to the case of high density of the defects in the case when defects are immobile), local crystallization of the passive matrix appears for a short time when the defect are in close vicinity and it relaxes back once particles move away (Movie S6).

Interestingly, the use of mobile defects can potentially lower the global density of the passive colloidal matrix needed to achieve the phase transition in comparison to the case of immobile defects. Namely, if two or more mobile defects move towards each other they can compress the matrix even if the initial particle density is too low to form a crystalline phase initially. In this situation, only local crystallites are formed, which are destroyed again, when at least one mobile defect is gone.

**Supplementary Movie files**

**Movie S1.** (for Figure 2a-d) Trajectory recordings of passive SiO<sub>2</sub> beads moving around a single Janus PS/Ag/AgCl particle under blue light illumination.

**Movie S2.** (for Figure. 3a-c) The Movie shows a phase transition in a system consisting of immobilized Janus particles (at low concentration with 2 active defects only) located at a dense passive matrix of SiO<sub>2</sub> beads. The measurement is carried out under blue light illumination.

**Movie S3.** (for Figure. 3d-f) The Movie shows a phase transition in a system consisting of immobilized Janus particles (at high concentration with 6 active defects) located at a dense passive matrix of SiO<sub>2</sub> beads. The measurement is carried out under blue light illumination.

**Movie S4.** Mobile single Janus particles moving under a passive matrix of SiO<sub>2</sub> beads.

**Movie S5.** Mobile double Janus particle moving under a passive matrix of SiO<sub>2</sub> beads.

**Movie S6.** The Movie shows a phase transition in a system consisting of double motile Janus particles located at a passive matrix of SiO<sub>2</sub> beads. The experiment is carried out under blue light illumination.

## References

- [1] Y. Bi, J. Ye, *Chem Commun (Camb)*. **2009**, DOI: 10.1039/b913725d6551.
- [2] J. Simmchen, A. Baeza, A. Miguel- Lopez, M. M. Stanton, M. Vallet-Regi, D. Ruiz-Molina, S. Sánchez, *ChemNanoMat*. **2017**, 3, 65.
- [3] a) A. Altemose, M. A. Sanchez-Farran, W. Duan, S. Schulz, A. Borhan, V. H. Crespi, A. Sen, *Angew. Chem. Int. Ed. Engl.* **2017**, 56, 7817; b) M. Ibele, T. E. Mallouk, A. Sen, *Angew. Chem. Int. Ed.* **2009**, 48, 3308; c) X. Wang, L. Baraban, V. R. Misko, F. Nori, T. Huang, G. Cuniberti, J. Fassbender, D. Makarov, *Small* **2018**, 1802537; d) V. Yadav, W. Duan, P. J. Butler, A. Sen, *Annu. Rev. Biophys.* **2015**, 44, 77.
- [4] C. Zhou, H. P. Zhang, J. Tang, W. Wang, *Langmuir* **2018**, 34, 3289.
- [5] a) N. N. Medvedev, A. Geiger, W. Brostow, *Int. J. Chem. Phys.* **1990**, 93, 8337; b) F. B. Usabiaga, D. Duque, *Phys. Rev. E*. **2009**, 79, 046709.